Nuclear Spins and Hyperfine-Structure Separations of Silver-112 and Silver-113*

YAU WA CHAN, W. BRUCE EWBANK,† WILLIAM A. NIERENBERG, AND HOWARD A. SHUGART
Department of Physics and Lawrence Radiation Laboratory, University of California, Berkeley, California
(Received 30 September 1963)

The nuclear spins and the hyperfine-structure separations in the $^2S_{1/2}$ electronic ground state of two silver isotopes, 3.2-h Ag^{112} and 5.3-h Ag^{113}, have been measured by the atomic-beam magnetic-resonance method. Combining these measurements with the known constants of Ag^{109}, the corresponding nuclear magnetic-dipole moments were calculated. The results are

Isotope	I	$\Delta\nu$(Mc/sec)	μ_I(uncorrected)nm
Ag^{112}	2	± 518.332 (18)	±0.0545 (5)
Ag^{113}	$\frac{1}{2}$	±2408.065 (28)	±0.158 (2)

The signs of the moments have not been determined in this experiment.

I. INTRODUCTION

THE atomic-beam magnetic-resonance technique employing the flop-in principle has been used[1,2] to measure the nuclear spins of 3.2-h Ag^{112} (Ref. 1) and 5.3-h Ag^{113} (Ref. 2) and their corresponding $^2S_{1/2}$ ground-state hyperfine-structure separations. The nuclear-magnetic moments have been calculated from the hyperfine-structure separations by using known properties of the stable isotopes for comparison. Resonances corresponding to the transitions of $\Delta F=0$ and $\Delta F=\pm 1$ were observed for both isotopes.

II. GENERAL PRINCIPLES

Knowledge of the nuclear properties investigated by the atomic-beam magnetic-resonance method is obtained by observing radio-frequency transitions between pairs of hyperfine sublevels of free atoms in a magnetic field. For a free atom of silver in the $^2S_{1/2}$ electronic ground state, the interaction of the nucleus with the s electron is limited to the contact magnetic interaction. In a magnetic field $\mathbf{H}$, the Hamiltonian of this isolated electronic-nuclear system may be written as

$$\mathcal{H}/h=-(g_J\mathbf{J}\cdot\mathbf{H}+g_I\mathbf{I}\cdot\mathbf{H})(\mu_0/h)+a(\mathbf{I}\cdot\mathbf{J}), \quad (1)$$

where $\mathbf{J}$ and $\mathbf{I}$ are the electronic and nuclear angular-momentum operators; g_J and g_I are the electronic and nuclear g factors, which relate the magnetic-dipole moments with the corresponding angular momenta by the equations $\boldsymbol{\mu}_J=g_J\mu_0\mathbf{J}$ and $\boldsymbol{\mu}_I=g_I\mu_0\mathbf{I}$; μ_0 is the magnitude of the Bohr magneton; a is the magnetic-dipole-interaction constant which is a measure of the strength of the magnetic-dipole hyperfine-structure interaction; and h is Planck's constant. The hyperfine-structure separation $\Delta\nu$ is related to the interaction constant by $\Delta\nu=a(I+\frac{1}{2})$. The constant a is approximately related to the atomic and nuclear g factors by[3]

$$a=-\frac{8\pi}{3}g_Ig_J\mu_0^2\rho_s(0), \quad (2)$$

where $\rho_s(0)$ is the electron density at the nucleus. In Eq. (2), the effects of the finite extent of the nuclear magnetism (hfs anomaly) and of the finite nuclear-charge distribution have been neglected. Since the electron density is approximately the same for two isotopes of the same element, the effect of the atomic electrons may be eliminated from Eq. (2) by considering ratios. The cancellation results in the Fermi–Segrè formula[4]

$$\frac{|g_I'|}{|g_I|}\approx\frac{|\Delta\nu'|(2I+1)}{|\Delta\nu|(2I'+1)}. \quad (3)$$

With this relationship, the g_I of an isotope can be calculated from the measured $\Delta\nu$, provided that both g_I' and $\Delta\nu'$ of another isotope of the same element have been determined. However, this method neglects the "hfs anomaly" (which amounts to 0.41%[5–7] between Ag^{107} and Ag^{109}) and does not permit one to determine the sign of g_I.

The analytic behavior of the energy levels for $J=\frac{1}{2}$ is described explicitly by the Breit–Rabi formula,[8] which may be written, in units of $h\Delta\nu$, as

$$W(x)/h\Delta\nu=-(\tfrac{1}{2}(2I+1))-(g_I/(g_I-g_J))m_Fx+(F-I)[1+(4m_F/(2I+1))x+x^2]^{1/2}, \quad (4)$$

where W is the energy of the state, $x=(-g_J+g_I)(\mu_0H/h\Delta\nu)$, F is the total angular-momentum quantum number, and m_F is its projection on the z axis. The energy-level diagrams for $x<2$ and for $I=2$ and $I=\frac{1}{2}$

* This research was supported in part by the U. S. Office of Naval Research and the U. S. Atomic Energy Commission.
† Present address: Nuclear Data Project, Oak Ridge National Laboratory, Oak Ridge, Tennessee.
[1] W. B. Ewbank, Y. W. Chan, and H. A. Shugart, Bull. Am. Phys. Soc. 6, 513 (1961).
[2] Y. W. Chan, W. B. Ewbank, W. A. Nierenberg, and H. A. Shugart, Bull. Am. Phys. Soc. 5, 503 (1960).
[3] Hans Kopfermann, *Nuclear Moments*, English translation by E. E. Schneider (Academic Press Inc., New York, 1958).
[4] E. Fermi and E. Segrè, Z. Physik 82, 729 (1933).
[5] G. Wessel and H. Lew, Phys. Rev. 92, 641 (1953).
[6] E. Brun, J. Oeser, H. H. Staub, and C. G. Telschow, Phys. Rev. 93, 172 (1954).
[7] P. Sogo and C. D. Jeffries, Phys. Rev. 93, 174 (1954).
[8] G. Breit and I. I. Rabi, Phys. Rev. 38, 2082 (1931).

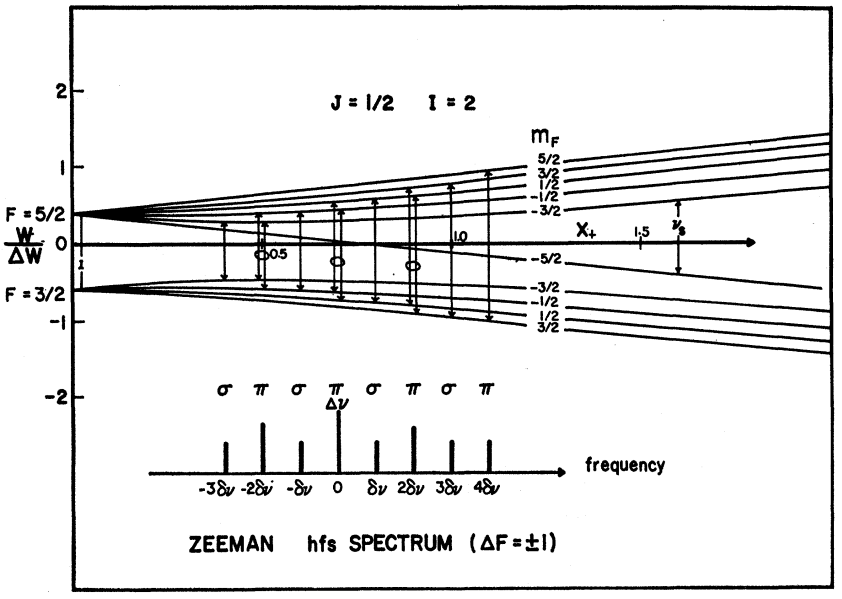

FIG. 1. Breit–Rabi energy diagram for $J=\frac{1}{2}$ and $I=2$, and the corresponding observable Zeeman spectrum at low magnetic field for $\Delta F=\pm 1$ transitions.

are shown in Figs. 1 and 2, respectively. In both diagrams, it is assumed that the nuclear magnetic moment is positive, $g_I>0$.

All measurements of transition frequencies in this experiment were performed at magnetic fields corresponding to $x<1$. In this region, the first-order selection rules $\Delta F=0$, $\Delta F=\pm 1$, and $\Delta m_F=0$, $\Delta m_F=\pm 1$ are applicable.[9] In a standard type of flop-in atomic-beam apparatus,[10] beams of neutral atoms pass a series of three magnets. The first and last magnetic fields (usually called A and B fields) are inhomogeneous and operate at a relatively high magnetic field, whereas the second field (C field) is homogeneous. An atom is refocussed and detected if and only if the sign of its effective magnetic moment in the B field is opposite to what it was in the A field. For atoms with $J=\frac{1}{2}$, this corresponds to a change of state from $m_J=\pm\frac{1}{2}$ to $m_J'=\mp\frac{1}{2}$, by an induced transition in the C-field region. In other words, the selection rule of the apparatus is equivalent to $\Delta m_J=\pm 1$.

The possible observable transitions at low magnetic field in an atom with $J=\frac{1}{2}$ may be summarized as follows: (a) For $\Delta F=0$, there is only one observable single-quantum transition corresponding to the transition $m_F=-I+\frac{1}{2}$ to $m_F'=-I-\frac{1}{2}$ for $F=I+\frac{1}{2}$. It is sometimes called the "standard transition." (b) For $\Delta F=\pm 1$ (usually called "direct transitions"), all transitions with $\Delta m_F=0$, $\Delta m_F=\pm 1$ are observable except the one from $m_F=-I-\frac{1}{2}$. For a given I, there are $6I-1$ observable direct transitions. Among these there are $2I-1$ pairs (doublets), the energies of which are so close (separation $\delta w=2\mu_0 g_I H$) as to be unresolved by an apparatus having a "poor" linewidth. Therefore, there are all together $4I$ observable $\Delta F=\pm 1$ resonances (lines). All observable transitions in the cases of $I=2$ and $I=\frac{1}{2}$ have been labeled in Figs. 1 and 2.

With the expansion of Eq. (4) in powers of x, the standard transition frequency ν_S and the direct transition frequencies ν_D at low magnetic field may be approximated by

$$\nu_S=(\nu_\infty+\nu_I)+2I(\nu_\infty^2/\Delta\nu)+\cdots \tag{5}$$

and

$$\nu_D=\Delta\nu+[(m_F+m_F')\nu_\infty+(m_F-m_F')\nu_I]+\cdots, \tag{6}$$

where $\nu_\infty\equiv x\Delta\nu/(2I+1)$ is the simple Zeeman frequency corresponding to $\Delta\nu=\infty$, and $\nu_I=-g_I(\mu_0/h)H$. When the magnetic field is low enough so that $\nu_\infty\ll\Delta\nu$ and when the small g_I terms are also neglected, Eq. (5) becomes

$$\nu_S\approx -g_J/(2I+1)(\mu_0/h)H. \tag{7}$$

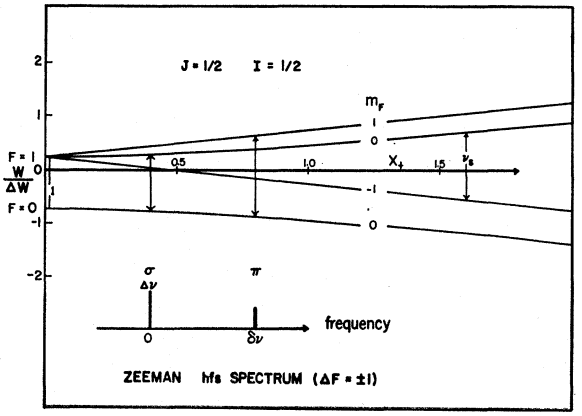

FIG. 2. Breit–Rabi energy diagram for $J=\frac{1}{2}$ and $I=\frac{1}{2}$ and the corresponding observable Zeeman spectrum at low magnetic field for $\Delta F=\pm 1$ transitions.

[9] P. Kusch and V. W. Hughes, in *Handbuch der Physik*, edited by S. Flügge (Springer-Verlag, Berlin, 1959), Vol. 37/1.
[10] J. R. Zacharias, Phys. Rev. **61**, 270 (1942).

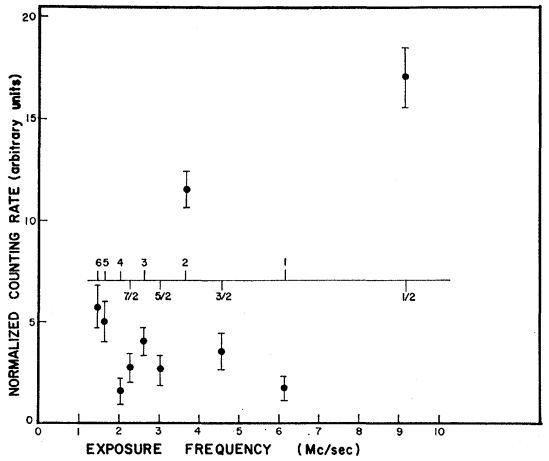

FIG. 3. Spin search of 3.2-h Ag^{112} and 5.3-h Ag^{113} from the reaction $Pd(\alpha; p,kn)Ag$.

This provides a simple relation for the nuclear-spin determination.

At higher magnetic field, the higher-order terms become important, and the hfs separation $\Delta\nu$ may be calculated from ν_S with an exact formula

$$\Delta\nu\delta\nu_S=(\nu_S-\nu_I)(-\nu_S+\nu_J), \quad (8)$$

where $\delta\nu_S=\nu_S-(\nu_\infty+\nu_I)$ is the deviation from the Zeeman frequency, and $\nu_J=-g_J(\mu_0/h)H$. The value of g_I needed for calculating ν_I is not known *a priori*, but it is related approximately to $\Delta\nu$ by Eq. (3). The smallness of the g_I term makes possible the calculation of $\Delta\nu$ and g_I by iterative procedures. Since the measurements of transition frequencies in this work were not accurate enough to establish the sign of g_I,[10,11] the final value of $\Delta\nu$ is obtained as the average value of two $\Delta\nu$'s that were calculated, respectively, by assuming a positive or negative sign for g_I. The main source of line-broadening in the apparatus used is the inhomogeneity of the C field. Therefore, the "direct transitions" provide the most accurate measurement of $\Delta\nu$, especially at a magnetic field at which one of the transition frequencies ν_D is not sensitive to changes in the magnetic field.

III. PRODUCTION OF SAMPLES

The samples of Ag^{112} and Ag^{113} used in this work were produced on the Berkeley 60-in. Crocker cyclotron by α bombardment of natural Pd foil. The palladium foil of 12-mil thickness was usually bombarded by 48-MeV α particles for 8 to 10 h at a beam level of about 50 μA. Since the abundance of Pd^{110} in natural palladium metal is only 11.8% and the cross section for the (α,p) and (α,pn) reactions is generally small, the activity of Ag^{112} and Ag^{113} was low. In addition to the desired reactions, there are others that are much more probable, e.g., $Pd(\alpha,kn)Cd$ for $k=1, 2, 3, 4$. In order to remove these contaminants, a chemical separation of silver from cadmium and from palladium was necessary. As a carrier solution for the silver chemistry, about 50 mg of silver carrier and 500 mg of cadmium carrier were dissolved in hot concentrated nitric acid. Weak hydrochloric acid was then added to precipitate silver chloride. The palladium target was dissolved in the solution by heating. After the solution was cooled to about 0°C, the AgCl precipitate was separated by centrifugation and was dissolved in 20 cc of hot solution of equal parts NaCN and NaOH. Pure aluminum-metal foil was used to reduce the silver to metallic form. The metallic silver was washed with distilled water and then dried.

IV. EXPERIMENTAL PROCEDURE

The atomic beam magnetic-resonance apparatus used and the general procedure employed for these measurements have been discussed elsewhere.[12,13] A standard tantalum oven was heated by electron bombardment to provide the source of beam atoms. Sulfur-coated buttons were used to collect radioactive atoms for the spin and resonance detection. After exposure, each button was counted in continuous-flow methane counters.

All data in each experimental run were corrected for counter background, for fluctuation of beam intensity,

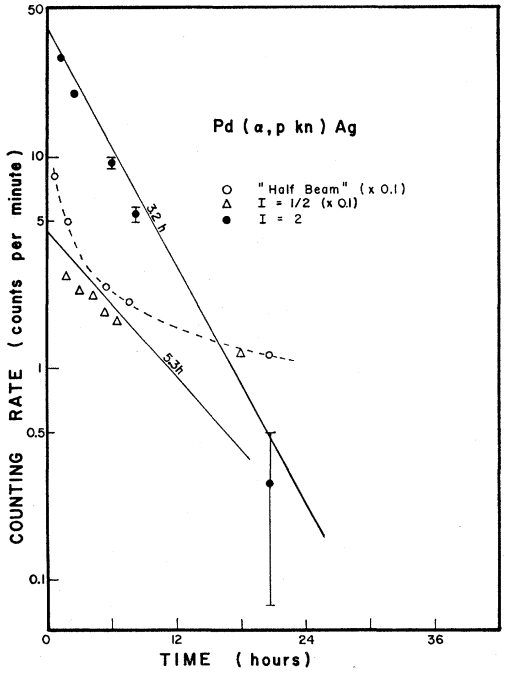

FIG. 4. A comparison of decay of beam activity and the decay of activities from the Ag sample for resonances of $I=\frac{1}{2}$ and $I=2$.

[11] N. F. Ramsey, *Molecular Beams* (Oxford University Press, London, 1956).

[12] J. P. Hobson, J. C. Hubbs, W. A. Nierenberg, H. B. Silsbee, and R. J. Sunderland, Phys. Rev. **104**, 101 (1956).

[13] W. B. Ewbank, L. L. Marino, W. A. Nierenberg, H. A. Shugart, and H. B. Silsbee, Phys. Rev. **120**, 1406 (1960).

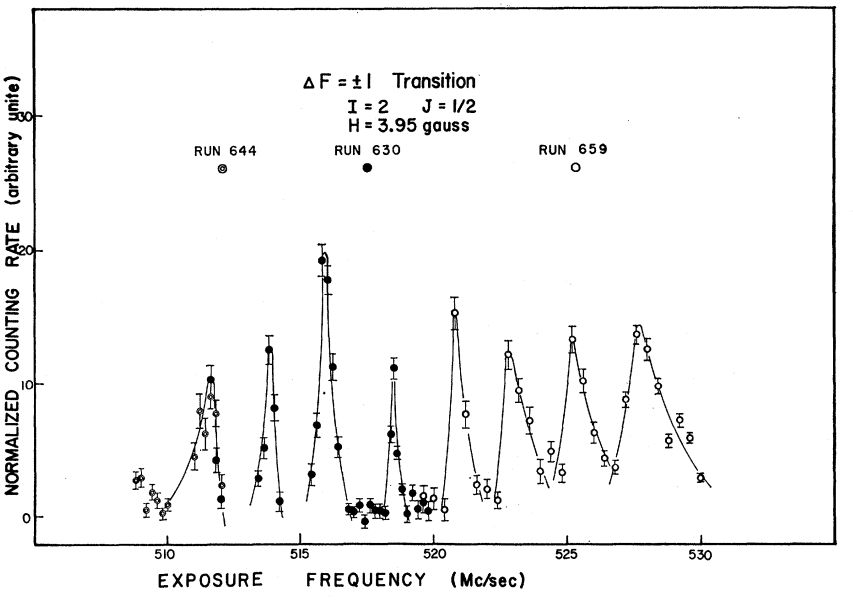

FIG. 5. Observed Zeeman spectrum of direct transitions in 3.2-h Ag^{112}.

and for radioactive decay as described in Ref. 13. The decay of each spin button or resonance-peak button was also used to establish the enrichment of the isotope studied. The transition magnetic field was calibrated by observing the "standard transition" in beams of Rb^{85} and Rb^{87}, which were detected by a surface-ionization detector.[14,15]

The radio-frequency oscillating magnetic field used for the induced transitions was produced by passing an rf current through a simple "strap hairpin" located in the C-field region. Frequencies in the range less than 40 Mc/sec were generated by a Tektronix 190 oscillator. A Hewlett-Packard 608A oscillator and two wide-band amplifiers (Instruments for Industries) provided enough power for the frequency range from 20 to 200 Mc/sec. Frequencies higher than 500 Mc/sec were generated by a Gertsch FM-4A oscillator (with frequency usually locked to a harmonic of the Gertsch AM-1, which was stabilized by a 100-kc/sec signal from a crystal-oscillator standard) and multiplied, if necessary, by a series of crystal harmonic generators. All frequencies less than 220 Mc/sec were monitored by a Hewlett-Packard 524B frequency counter with 525A and 525B frequency converters. For frequencies above 200 Mc/sec, the HP-540A transfer oscillator was also used. A crystal oscillator (James Knight Company JKFS-1100) was used as a secondary frequency standard and was checked periodically with a National Company Atomichron. The input rf power was monitored by a HP-430 power meter.

For a given isotope, all resonance frequencies corresponding to different transitions and different magnetic fields were analyzed by a digital-computer program to give a best-fit value of $\Delta\nu$ according to the method of least squares.[16] In order to allow for the possibility of systematic errors in the apparatus, the uncertainty assigned for the best-fit value of $\Delta\nu$ is taken to be twice the standard deviation resulting from the least-squares analysis.

V. RESULTS FOR SILVER-112

The results of a spin-search experiment for the silver sample produced by the reactions $Pd(\alpha; p,kn)$ are shown in Fig. 3. Signals at $I=2$ and $I=\frac{1}{2}$ were observed. The decay of these activities is shown in Fig. 4. The decay curve for $I=2$ shows an enrichment of 3.2-h Ag^{112}. In this way, the spin assignment $I=2$ for Ag^{112} was first established. Several resonances of the standard transition were observed at higher magnetic fields for $I=2$. A calculation from these resonances indicated that the $\Delta\nu$ of Ag^{112} was about 518(2) Mc/sec. In this frequency range, the observation of direct transitions is rather simple. The $\Delta F=\pm 1$ resonances of the hfs Zeeman spectrum predicted in Fig. 1 are shown in Fig. 5. The resonance $(\frac{5}{2}, -\frac{1}{2}) \leftrightarrow (\frac{3}{2}, -\frac{3}{2})$ was also observed at a field of ≈ 77G where $\partial\nu/\partial H=0$. This field-independent resonance gives the most accurate measurement of $\Delta\nu$ and is shown in Fig. 6.

Details of all observations for Ag^{112} are listed in Table I. With these data, the best-fit value of $\Delta\nu$, calculated by assuming $\mu_I>0$ or $\mu_I<0$, is also given. Since the difference between the two calculated $\Delta\nu$'s is much smaller than either of their errors, the measurement in this experiment is not precise enough to tell the sign of the magnetic-dipole moment. We will take the average value to represent the final result for $\Delta\nu$,

$$\Delta\nu(Ag^{112}) = \pm 518.332(18).$$

[14] J. B. Taylor, Phys. Rev. **35**, 375 (1930).
[15] E. Langmuir and K. H. Kingdon, Proc. Roy. Soc. (London) **A107**, 61 (1925).
[16] F. R. Petersen and H. A. Shugart, Phys. Rev. **125**, 284 (1962).

TABLE I. Ag^{112} data.

Run	Calibration isotope and frequency (Mc/sec) Rb^{85}	Rb^{87}	H (G)	F_1	m_1	F_2	m_2	ν_{obs} (Mc/sec)	Residual (kc/sec)	Weight factor
6101	4.685 (20)	6.984 (25)	9.956 (9)	$\frac{5}{2}$	$-\frac{3}{2}$	$\frac{5}{2}$	$-\frac{5}{2}$	5.825 (30)	−4	1075
6102	9.575 (10)	14.207 (10)	20.188 (15)	$\frac{5}{2}$	$-\frac{3}{2}$	$\frac{5}{2}$	$-\frac{5}{2}$	12.373 (40)	1	588
6161	38.358 (20)	55.379 (20)	77.314 (30)	$\frac{5}{2}$	$-\frac{3}{2}$	$\frac{5}{2}$	$-\frac{5}{2}$	61.825 (50)	21	280
6162	91.739 (20)	126.446 (30)	171.362 (6)	$\frac{5}{2}$	$-\frac{3}{2}$	$\frac{5}{2}$	$-\frac{5}{2}$	204.920 (100)	10	99
6241	1.237 (10)	1.802 (10)	2.609 (50)	$\frac{5}{2}$	$\frac{1}{2}$	$\frac{3}{2}$	$\frac{3}{2}$	521.500 (200)	201	23
6242	1.239 (10)	1.804 (10)	2.613 (50)	$\frac{5}{2}$	$\frac{1}{2}$	$\frac{3}{2}$	$\frac{1}{2}$	520.000 (200)	165	25
6243	1.241 (10)	1.806 (10)	2.616 (50)	$\frac{5}{2}$	$-\frac{1}{2}$	$\frac{3}{2}$	$\frac{1}{2}$	518.400 (50)	18	399
6244	1.243 (10)	1.808 (10)	2.620 (50)	$\frac{5}{2}$	$-\frac{1}{2}$	$\frac{3}{2}$	$-\frac{1}{2}$	517.000 (100)	86	94
6245	1.245 (10)	1.810 (10)	2.623 (50)	$\frac{5}{2}$	$-\frac{3}{2}$	$\frac{3}{2}$	$-\frac{1}{2}$	515.400 (150)	−33	39
6246	1.247 (10)	1.812 (10)	2.627 (50)	$\frac{5}{2}$	$-\frac{3}{2}$	$\frac{3}{2}$	$-\frac{3}{2}$	514.000 (100)	51	59
6301	1.924 (10)	2.883 (17)	4.112 (7)	$\frac{5}{2}$	$-\frac{1}{2}$	$\frac{3}{2}$	$\frac{1}{2}$	518.500 (50)	44	400
6302	1.919 (10)	2.869 (17)	4.097 (7)	$\frac{5}{2}$	$-\frac{1}{2}$	$\frac{3}{2}$	$-\frac{1}{2}$	515.900 (200)	259	25
6303	1.914 (10)	2.855 (17)	4.082 (7)	$\frac{5}{2}$	$-\frac{1}{2}$	$\frac{3}{2}$	$-\frac{3}{2}$	513.850 (150)	−8	44
6441	1.860 (10)	2.758 (10)	3.955 (20)	$\frac{5}{2}$	$-\frac{1}{2}$	$\frac{3}{2}$	$\frac{1}{2}$	518.428 (40)	−18	625
6442	1.861 (10)	2.760 (10)	3.958 (20)	$\frac{5}{2}$	$-\frac{3}{2}$	$\frac{3}{2}$	$-\frac{3}{2}$	511.600 (200)	−154	24
6591	1.860 (5)	2.754 (5)	3.952 (20)	$\frac{5}{2}$	$-\frac{1}{2}$	$\frac{3}{2}$	$\frac{1}{2}$	518.454 (20)	7	2492
6592	1.860 (5)	2.754 (5)	3.952 (20)	$\frac{5}{2}$	$\frac{1}{2}$	$\frac{3}{2}$	$\frac{1}{2}$	520.700 (150)	39	44
6593	1.860 (5)	2.754 (5)	3.952 (20)	$\frac{5}{2}$	$\frac{1}{2}$	$\frac{3}{2}$	$\frac{3}{2}$	522.900 (250)	43	16
6594	1.860 (5)	2.754 (5)	3.952 (20)	$\frac{5}{2}$	$\frac{3}{2}$	$\frac{3}{2}$	$\frac{3}{2}$	525.200 (200)	145	24
6595	1.860 (5)	2.754 (5)	3.952 (20)	$\frac{5}{2}$	$\frac{5}{2}$	$\frac{3}{2}$	$\frac{3}{2}$	527.550 (300)	319	11
7191	38.485 (25)	55.579 (25)	77.571 (25)	$\frac{5}{2}$	$-\frac{1}{2}$	$\frac{3}{2}$	$-\frac{3}{2}$	472.762 (10)	5	10 000

Calibration and comparison information:

Isotope	Spin	g_J	$\Delta\nu$ (Mc/sec)	μ_I (uncorr) nm[a]
Rb^{85}[b]	$\frac{5}{2}$	−2.002409	3035.732	+1.34817
Rb^{87}[b]	$\frac{3}{2}$	−2.002409	6834.683	+2.7413
Ag^{109}[c]	$\frac{1}{2}$	−2.0023612	−1976.932	−0.129931

Summary of results:

Ag^{112}	$I=2$	$\Delta\nu=+518.333$ (18) $=-518.331$ (18)	μ_I (uncorr) $=\pm0.0545$ (5)	$\chi^2=8.2$ if positive moment $=8.6$ if negative moment

[a] I. P. K. Lindgren, University of Uppsala, Uppsala, Sweden (private communication, August 1963).
[b] S. Penselin, T. Moran, V. W. Cohen, and G. Winkler, Phys. Rev. **127**, 524 (1962).
[c] S. Penselin, Physikalische Institute, University of Heidelberg, Germany (private communication, August 1963).

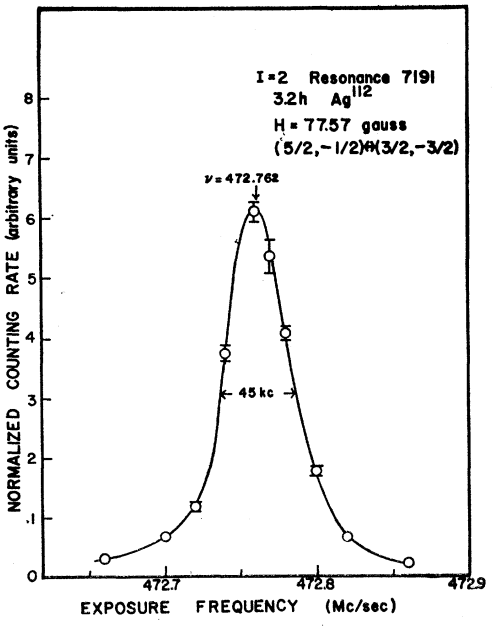

FIG. 6. Field-independent resonance of direct transition in 3.2-h Ag^{112}.

With Ag^{109} as a comparison isotope, the μ_I of Ag^{112} calculated by the Fermi–Segrè formula is

$$\mu_{I(\text{uncorr})}(Ag^{112})=\pm0.0545(5)\text{ nm},$$

where 1% uncertainty has been assigned to the result and is meant to include a possible hfs anomaly.

VI. RESULTS FOR SILVER-113

The spins of all the silver isotopes of odd mass number from Ag^{105} to Ag^{111} have been determined to be $I=\frac{1}{2}$ (Refs. 17–19), arising from the unpaired $p_{1/2}$ proton. Therefore, the spin of Ag^{113} is also expected to be $I=\frac{1}{2}$. Since the measured magnetic-dipole moments of these odd-A isotopes are quite similar,[6,7,20,21] the

[17] D. A. Jackson and H. Kuhn, Proc. Roy. Soc. (London) **A158**, 372 (1937).
[18] W. B. Ewbank, W. A. Nierenberg, H. A. Shugart, and H. B. Silsbee, Phys. Rev. **110**, 595 (1958).
[19] A. Lemonick and F. M. Pipkin, Phys. Rev. **95**, 1356 (1954).
[20] W. B. Ewbank and H. A. Shugart, Phys. Rev. **129**, 1617 (1963).
[21] G. K. Woodgate and R. W. Hellwarth, Proc. Phys. Soc. (London) **69A**, 581 (1956); Nature **176**, 395 (1955).

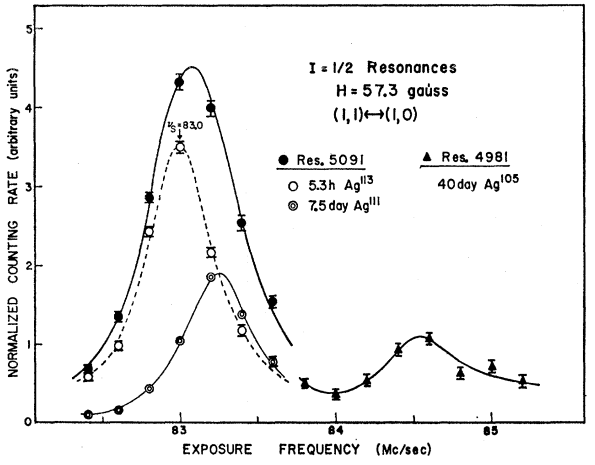

FIG. 7. Resonance of standard transition for 40-day Ag^{105} 7.5-day Ag^{111}, and 5.3-h Ag^{113}. The resonances of Ag^{111} and Ag^{113} were resolved by radioactive decay analysis.

dipole moment of Ag^{113} may be expected to have about the same magnitude.

As shown in Fig. 3, a strong signal of $I=\frac{1}{2}$ was observed in the spin-search experiment. The decay curve of this activity (shown in Fig. 4) indicated an enrichment of 5.3-h activity during the first six hours, and then a transition to an activity with a much longer half-life. This shows that the signal of $I=\frac{1}{2}$ could be the result of a mixture of Ag^{113}, Ag^{111}, and Ag^{105}. Several resonances were observed at higher magnetic fields. In general, the buttons exposed on the low-frequency side of the resonance decayed faster than those exposed on the high-frequency side. After decay fitting, the resonances of Ag^{111} and Ag^{113} were resolved at approx 57G as shown in Fig. 7. The resonance 4981 was identified as being due to Ag^{105}. A resonance of Ag^{113} at $H\approx 552$ G is shown in Fig. 8. The decay curve of the peak activity is shown in Fig. 9, in which an enrichment of 5.3-h Ag^{113} activity was identified. By this stage, the spin assignment of $I=\frac{1}{2}$ for Ag^{113} was established, and the calculated $\Delta\nu$ was good enough for a direct-transition search.

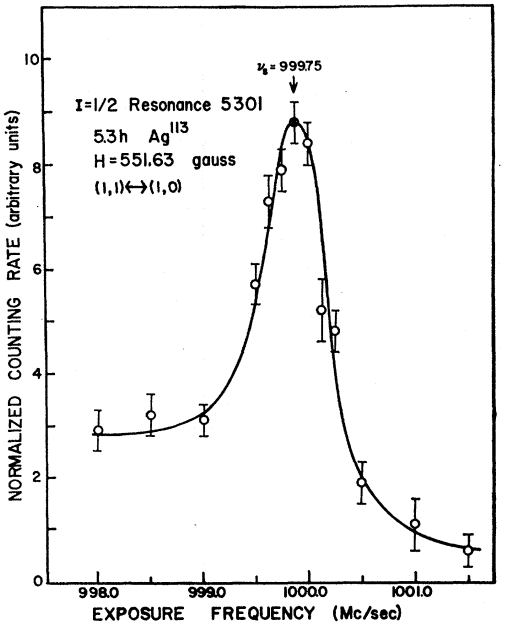

FIG. 8. Resonance of the standard transition in 5.3-h Ag^{113}.

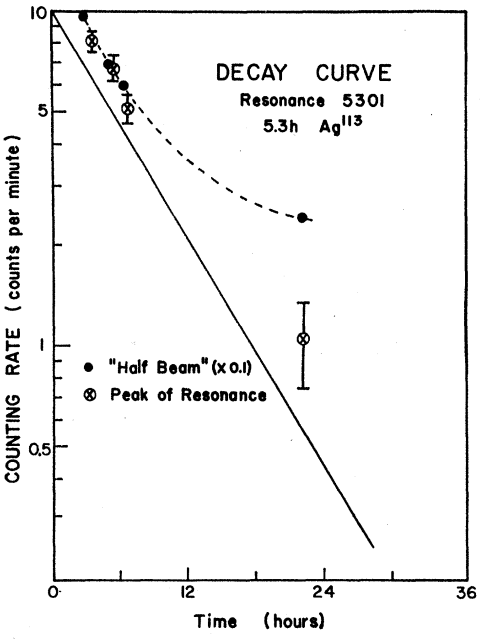

FIG. 9. A decay comparison of the beam activity and the "peak activity of a 5.3-h Ag^{113} resonance.

The direct transitions for this isotope are shown in Fig. 10. The central dip of the σ transition ($\Delta m_F=0$) is due to the effect of two oppositely directed rf fields around the single wire-strap hairpin.

A summary of the experimental data and calculated

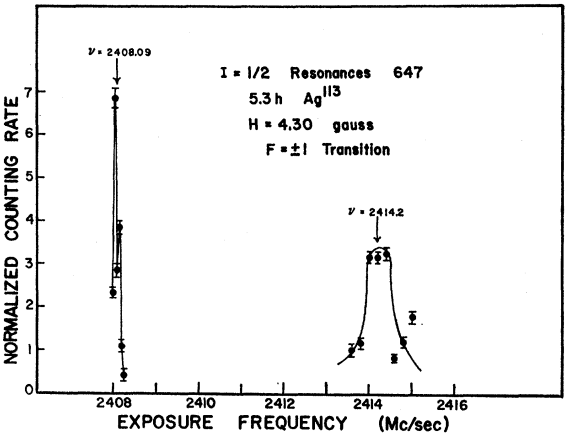

FIG. 10. Observed Zeeman spectrum of direct transition in 5.3-h Ag^{113}.

TABLE II. Ag^{113} data. (Calibration and comparison information is the same as in Table I.)

Run	Calibration isotope and frequency (Mc/sec) Rb^{85}	Rb^{87}	H (G)	F_1	m_1	F_2	m_2	ν_{obs} (Mc/sec)	Residual (kc/sec)	Weight factor
5091	27.960 (30)	40.783 (40)	57.276 (30)	1	0	1	−1	83.000 (100)	58	83
5151	74.274 (20)	103.973 (15)	142.159 (35)	1	0	1	−1	215.600 (150)	5	38
5181	196.855 (15)	250.178 (5)	323.202 (20)	1	0	1	−1	535.150 (300)	−155	11
5301	411.320 (10)	459.962 (10)	551.630 (10)	1	0	1	−1	999.750 (350)	−83	16
6471	2.023 (7)	3.006 (5)	4.305 (10)	1	0	0	0	2408.090 (20)	−5	2500
6472	2.023 (7)	3.006 (5)	4.305 (10)	1	0	0	0	2408.100 (20)	5	2500
6473	2.023 (7)	3.006 (5)	4.305 (10)	1	1	0	0	2414.200 (200)	86	25

Summary of results:

Ag^{113}	$I=\frac{1}{2}$	$\Delta\nu=\pm2408.065$ (28) Mc/sec	μ_I(uncorr) $=\pm0.158$ (2) nm	$\chi^2=0.9$ for + moment $=1.0$ for − moment

results for Ag^{113}, similar to that for Ag^{112}, is shown in Table II. The same value of $\Delta\nu$ is obtained by assuming either sign of g_I. The best value of $\Delta\nu$ is

$$\Delta\nu(Ag^{113})=\pm2408.065(28)\ \text{Mc/sec}.$$

From the Fermi-Segrè formula, we have

$$\mu_{I(\text{uncorr})}(Ag^{113})=\pm0.158(2)\ \text{nm}.$$

The assignment of errors is the same as for Ag^{112}.

VII. DISCUSSION

The measured nuclear spin $I=\frac{1}{2}$ for Ag^{113} indicates that $2p_{1/2}$ is the shell-model assignment for the odd proton. It is interesting to see that the absolute value of the nuclear magnetic-dipole moments of the odd silver isotopes from Ag^{105} to Ag^{113} increase almost linearly with neutron number, as is shown in Fig. 11. Because the nuclear properties of these odd silver isotopes are similar, the sign of the magnetic moment of Ag^{113} is probably the same as for Ag^{107} and Ag^{109}, which are known to be negative.

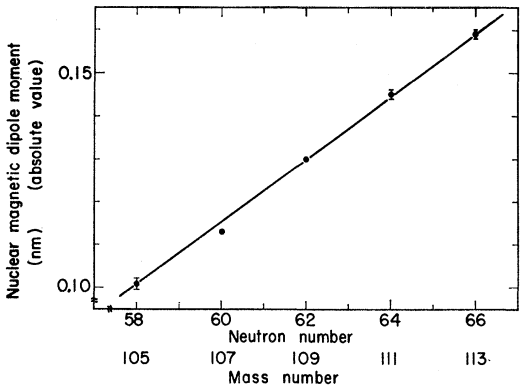

FIG. 11. A comparison of magnetic dipole moments for the silver odd isotopes from Ag^{105} to Ag^{113}.

Since the measured magnetic-dipole moment is so small and also, so far as is known, there is no isomeric state for Ag^{112}, it appears that the neutron-proton coupling in Ag^{112} may be quite different from that of $Ag^{104,106,108,110}$ (Refs. 18 and 22). The shell model[23] predicts close competition between the $2p_{1/2}$ and $1g_{9/2}$ orbitals from 39 to 49 protons, and also among $2d_{5/2}$, $1g_{7/2}$, and $1h_{11/2}$ from 51 to 75 neutrons. Assuming that the pairing energy favors low j values, the $I=2$ for Ag^{112} may be explained as the result of coupling of $\pi(p_{1/2})\nu(d_{5/2})^{-1}$, according to Nordheim's "strong rule."[24]

The magnetic moment of this configuration would be -1.61 nm if the magnetic moments of the free proton ($+2.79$ nm) and neutron (-1.91 nm) were used. However, the magnetic moment of Cd^{109} ($I=\frac{5}{2}$, $\mu=-0.829$ nm)[25] indicates considerable quenching[26] for the $d_{5/2}$ neutron. Using the empirical moments for the $d_{5/2}$ neutron in Cd^{109} and the $p_{1/2}$ proton in Ag^{113}, we find that the j–j coupling shell model predicts $\mu=-0.67$ nm for the $\pi(p_{1/2})\nu(d_{5/2})^{-1}$ configuration. Although the measured nuclear moment is much smaller, no other combination of the possible single-particle states fits the result as well.

[22] O. Ames, A. M. Bernstein, M. H. Brennan, and D. R. Hamilton, Phys. Rev. **123**, 1793 (1961); W. B. Ewbank, L. L. Marino, W. A. Nierenberg, H. A. Shugart, and H. B. Silsbee, Phys. Rev. **115**, 614 (1959).

[23] M. G. Mayer and J. H. D. Jensen, *Elementary Theory of Nuclear Shell Structure* (John Wiley & Sons, Inc., New York, 1955).

[24] L. W. Nordheim, Phys. Rev. **78**, 294 (1950).

[25] M. N. McDermott and R. Novick, Phys. Rev. **131**, 707 (1963).

[26] F. Bloch, Phys. Rev. **83**, 839 (1951).